Personalized phenotype encoding and prediction of pathological development from cross-sectional images.

Connor Elkhill*, Ines. A Cruz-Guerrero, PhD*, Jiawei Liu, MS*, Marius George Linguraru, DPhil†, Allyson Alexander, MD§, Brooke French, MD¶, Antonio R. Porras, PhD *
*Department of Biostatistics and Informatics, Colorado School of Public Health, Aurora, CO
†Sheikh Zayed Institute for Pediatric Surgical Innovation, Children's National Hospital, Washington, DC
‡Departments of Radiology and Pediatrics,George Washington University
School of Medicine and Health Sciences, Washington, DC
§Department of Pediatric Neurosurgery, Children's Hospital Colorado, Aurora, CO
¶Department of Pediatric Plastic and Reconstructive Surgery, Children's Hospital Colorado, Aurora, CO
‖Departments of Pediatrics, Surgery and Biomedical Informatics, School of Medicine, Aurora, CO
Email: connor.2.elkhill@cuanschutz.edu

***Abstract*—The prediction of anatomical development plays a crucial role in pediatric treatment selection and planning. We present a novel deep learning architecture to make personalized predictions of pediatric normative and pathologic head development using only cross-sectional data. We designed growth predictor that learns the anatomical effects of age and sex in the presence of pathology and a novel phenotype encoder that utilizes domain adversarial training to create age- and sex-independent representations of patient phenotypes. We combined these modules to instantiate patient phenotypes to specific ages for personalized anatomical predictions conditioned to cranial pathology. We trained our models using standardized head segmentations generated from cross-sectional CT images and 3D photograms and evaluated model performance using an independent longitudinal dataset of normative subjects and children with craniosynostosis. The model achieved a head surface growth prediction error of 4.93 ± 2.29 mm and a volumetric error 0.17 ± 0.11 L in patients with cranial pathology, and 4.61 ± 3.28 mm and 0.27 ± 0.19 L for normative subjects, demonstrating state-of-the-art accuracy. Our method is the first to create age- and sex-agnostic phenotypical representations and enable personalized predictions of pathological development from only cross-sectional data.**

***Index Terms*—predictive growth, craniosynostosis, generative adversarial network, domain adversarial training, pediatric pathological development**

I. Introduction

Children undergo a rapid cranial and brain growth during the first few years of life that is crucial for their cognitive development [1]. Craniosynostosis is a condition where one or more of the cranial sutures fuse prematurely and constrain cranial and brain development, often requiring surgical intervention [2]. However, current clinical standards to evaluate developmental anomalies rely on normative growth charts of simple metrics such as head circumference, cephalic index, or intracranial volume [3]–[5] that cannot characterize or predict development of patients with pathology [6]–[8].

Several methods to predict cranial growth without longitudinal training datasets have recently been proposed. Liu et al [9] created a normative reference of cranial growth based on age and sex using principal component analysis and temporal regression. However, this method is not personalized and only identified average growth trajectories in the normative pediatric population. Porras et al [10] presented a personalized predictive model of cranial growth, but the optimization was not computationally feasible for large datasets. Recently, Liu et al [11] presented a data-driven model of cranial suture growth trained only with cross-sectional data, and demonstrated state-of-the-art accuracy to predict pathologic development in patients with craniosynostosis. However, this method required the observation of the cranial sutures from computed tomography (CT) images, an image modality that requires harmful radiation exposure [12]. In a different domain, Xia et al [13] utilized generative adversarial networks to learn subject-specific trajectories from a cross-sectional dataset of magnetic resonance (MR) images to predict changes in the brain morphology of patients with Alzheimer's disease. However, their paired training scheme prevented significant anatomical temporal changes, which provided good results in adults but is not realistic in children [14].

As an alternative to CT imaging, 3D photogrammetry has become a popular radiation-free and low-cost clinical alternative to evaluate pediatric cranial malformations [15], [16]. However, it can only image the head surface and hence, prior personalized methods [11] relying on the identification of the cranial sutures are not feasible. We present a novel deep learning architecture designed to make personalized predictions of normative and pathologic development trained using head surface information from both cross-sectional CT images and 3D photograms, which enables radiation-free

Identify applicable funding agency here. If none, delete this.

prediction of pediatric development in a clinical setting. We propose a temporal growth predictor based on a conditional generative adversarial network that learns age- and sex - specific anatomical distributions with or without the presence of pathology in the pediatric population. We also present a novel phenotype encoder that utilizes domain adversarial training, avoiding the stringent statistical assumptions of prior works, to generate age- and sex-agnostic latent representations of patient phenotypes. These modules work collaboratively to generate personalized predictions of anatomical development by instantiating patient-specific phenotype representations to specific ages conditioned to the presence of pathology. The architecture was trained using only cross-sectional data from normative children and patients with craniosynostosis under the age of 10 years and was evaluated using an independent longitudinal dataset.

II. Materials and Methods

A. Data

After IRB approval at XXXXXXXXXXXXXXXXX (#XXXXXXXXXXXXXXXX) we collected two independent retrospective datasets: (1) a cross-sectional dataset used for model training; and (2) a longitudinal dataset used for performance evaluation. **Dataset 1** includes 2,672 cross-sectional CT images (N=2,262) and 3D photograms (N=410) of two patient populations: 2,020 normative subjects without cranial pathology (1081 male, 939 female, age 3.14 ± 3.05 years, range 0-10 years) and 652 patients with craniosynostosis (384 male, 268 female, age 0.64 ± 1.04 years, range 0-8.8 years). Dataset 2 includes two groups of longitudinal images: 61 CT image pairs from 51 normative subjects (28 male, 23 female) with average age at first image 2.24 ± 2.22 years and age at second image 3.55 ± 2.71 years (five subjects had two image pairs); and 75 pairs of 3D photograms from 75 patients with craniosynostosis (58 male, 17 female), with age of 0.61 ± 1.07 years at the first image and 0.85 ± 1.18 years at the second image.

B. Standard representation of the head surface

We used publicly available methods to segment the head surface from CT images and 3D photograms and create standardized 2D anatomical representations [10]. In summary, adaptive thresholding [9] and the marching cubes algorithm [18] were used to segment the head surface from a CT image. Four cranial landmarks were automatically identified at the glabella, two temporal processes of the dorsum sellae and the opisthion in CT images. In 3D photogrammetry, we used a similar publicly available method to identify a series of anatomical landmarks on the head and face [17]. We used a standardized template image annotated with both sets of landmarks to align the images from both modalities given their respective landmarks. We segmented the calvaria from the rest of the head at the cranial base using the plane defined by the nasion, left and right tragion annotated on the standardized template (Fig 1b). Finally, the head surface segmented from either image modality was sampled in spherical coordinates to create a standard 2D representation [10] Fig 1c.

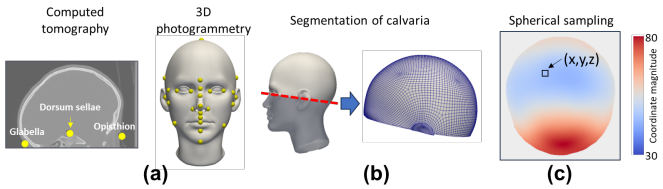

Fig. 1. Standard representation of the head surface. (a) CT image or 3D photogram annotated with anatomical landmarks. Detailed annotations of landmarks for 3D photograms can be found in [17]. (b) Segmented head surface using the naso-tragal plane. (c) Two-dimensional standard representation of the head surface using spherical sampling, where each pixel contains the corresponding location in the head surface (X, Y, Z).

C. Model architecture

We propose a neural network architecture composed of two main modules as presented in 2 and described below. Personalized phenotype encoder (PPE). The goal of this module is to create a vectorized representation of the head phenotype of a patient independently from age and sex. To accomplish this, we designed a phenotype encoder that uses unsupervised representation learning and the convolutional architecture presented in [19] to provide a latent patient-specific phenotype representation $\mathbf{l}$ based on a real head shape observation $\mathbf{X}$. Unlike previous work, we incorporate an additional phenotype discriminator (PD, purple in 2) and use a domain adversarial training scheme [20] (see details in section 2.4, Eq. 1)to promote a phenotype representation $\mathbf{l}$ that is independent from age or sex. Hence, the encoder will learn to generate latent phenotype representations $\mathbf{l}$ that cannot be used by the PD to identify the age and sex of the patient. Growth predictor (GP). This module uses an adversarial training scheme with the goal of generating a realistic head surface anatomy from a latent representation of a head phenotype $\mathbf{l}$ (generated by the PPE) together with information about age, sex and pathology by leveraging the learned anatomical distributions of specific patient groups in the training dataset. The GP and PPE work collaboratively to create personalized latent phenotype representations that are age- and sex-agnostic and that, when combined with specific age, sex, and pathology information, can represent the head anatomy of a specific patient. The predictor follows the convolutional architecture proposed by [19] but it was modified to include the conditions of patient age (encoded as a continuous variable), sex (binary encoded) and suture fusion status (one-hot encoded). Finally, the growth discriminator (GD) (Fig 2, in green) enables adversarial training of both the GP and PPE. The discriminator also utilizes the convolutional architecture proposed in [19] to compute the Wasserstein distance [21] and distinguish between real head shapes and head shapes reconstructed from $\mathbf{l}$.

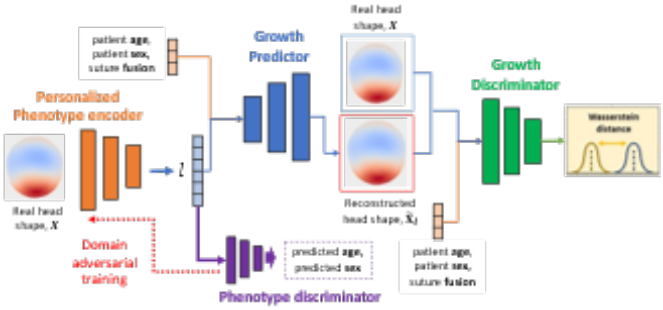

Fig. 2. Proposed neural network architecture. The personalized phenotype encoder creates a latent representation of a patient phenotype l from a real head shape that is independent of patient age or sex using domain-adversarial training. The growth predictor is trained to predict head anatomies consistent with the observed statistical distributions in the population for specific age, sex, and suture fusion status. Once trained, the phenotype representation of a patient l can be instantiated at any age using the growth predictor to produce personalized predictions.

D. Optimization

We defined the prediction of age and sex from the PD as $S', A' = PD(l; \theta_{PD})$ respectively, where θ_{PD} are the learned parameters of the PD and **l** is the latent representation generated from the PPE using real input image **X**. Similar to [22], we computed the cross entropy between S and S' and KL divergence between the continuous distributions of A and A', where A and S are the true patient age and sex. The PPE and PD modules are trained using the following adversarial loss function:

$$L_{PPE} = \max_{PPE} \min_{PD} S * log(S') + (1 - S) * log(1 - S') + A * log\frac{A}{A'} \quad (1)$$

To train the GP module, we used an adversarial scheme with the following Wasserstein loss function [21].

$$L_{GP} = E_{X^- \ P_l | X_{P_x}} \quad (2)$$

REFERENCES

[1] M. Cao, H. Huang, and Y. He, "Developmental connectomics from infancy through early childhood," *Trends in Neurosciences*, vol. 40, pp. 494–506, 8 2017.

[2] I. M. Mathijssen, "Updated guideline on treatment and management of craniosynostosis," *Journal of Craniofacial Surgery*, vol. 32, pp. 371–450, 1 2021.

[3] W. Likus, G. Bajor, K. Gruszczyńska, J. Baron, J. Markowski, M. Machnikowska-Sokołowska, D. Milka, and T. Lepich, "Cephalic index in the first three years of life: Study of children with normal brain development based on computed tomography," *The Scientific World Journal*, vol. 2014, p. 502836, 2 2014. publisher: Hindawi Publishing Corporation.

[4] P. Meyer-Marcotty, H. Bohm, C. Linz, J. Kochel, A. Stellzig-Eisenhauer, and T. Schweitzer, "Three-dimensional analysis of cranial growth from 6 to 12 months of age," *The European Journal of Orthodontics*, vol. 36, pp. 489–496, 10 2014.

[5] J. D. Rollins, J. S. Collins, and K. R. Holden, "United states head circumference growth reference charts: Birth to 21 years," *The Journal of Pediatrics*, vol. 156, pp. 907–913.e2, 6 2010.

[6] R. Breakey, P. G. Knoops, A. Borghi, N. Rodriguez-Florez, J. O'Hara, G. James, D. J. Dunaway, S. Schievano, and N. O. Jeelani, "Intracranial volume and head circumference in children with unoperated syndromic craniosynostosis," *Plastic and reconstructive surgery (1963)*, vol. 142, no. 5, pp. 708e–717e, 2018. publisher-place: United States publisher: United States: American Society of Plastic Surgeons.

[7] S. Sgouros, "Skull vault growth in craniosynostosis," *Child's Nervous System*, vol. 21, pp. 861–870, 10 2005.

[8] P. A. Thakkar, K. Yagnik, N. T. Parmar, R. R. Das, and U. P. Thakkar, "Observer variability in head circumference measurement using routine versus non-stretchable tapes in children," *Journal of Nepal Paediatric Society*, vol. 37, pp. 238–243, 6 2018.

[9] J. Liu, C. Elkhill, S. LeBeau, B. French, N. Lepore, M. G. Linguraru, and A. R. Porras, "Data-driven normative reference of pediatric cranial bone development," *Plastic and Reconstructive Surgery - Global Open*, vol. 10, p. e4457, 8 2022.

[10] A. R. Porras, R. Keating, J. Lee, and M. G. Linguraru, "Predictive statistical model of early cranial development," *IEEE Transactions on Biomedical Engineering*, vol. 69, pp. 537–546, 2 2022.

[11] J. Liu, J. H. Froelicher, B. French, M. G. Linguraru, and A. R. Porras, "Data-driven cranial suture growth model enables predicting phenotypes of craniosynostosis," *Scientific Reports*, vol. 13, p. 20557, 11 2023.

[12] T. Schweitzer, H. Böhm, P. Meyer-Marcotty, H. Collmann, R.-I. Ernestus, and J. Krauß, "Avoiding ct scans in children with single-suture craniosynostosis," *Child's Nervous System*, vol. 28, pp. 1077–1082, 7 2012.

[13] T. Xia, A. Chartsias, C. Wang, and S. A. Tsaftaris, "Learning to synthesise the ageing brain without longitudinal data," *Medical Image Analysis*, vol. 73, p. 102169, 10 2021.

[14] C. Hasegawa, T. Takahashi, Y. Yoshimura, S. Nobukawa, T. Ikeda, D. N. Saito, H. Kumazaki, Y. Minabe, and M. Kikuchi, "Developmental trajectory of infant brain signal variability: A longitudinal pilot study," *Frontiers in Neuroscience*, vol. 12, p. 566, 8 2018.

[15] A. R. Porras, L. Tu, D. Tsering, E. Mantilla, A. Oh, A. Enquobahrie, R. Keating, G. F. Rogers, and M. G. Linguraru, "Quantification of head shape from three-dimensional photography for presurgical and postsurgical evaluation of craniosynostosis:," *Plastic and Reconstructive Surgery*, vol. 144, pp. 1051e–1060e, 12 2019.

[16] T. Abdel-Alim, R. Iping, E. B. Wolvius, I. M. Mathijssen, C. M. Dirven, W. J. Niessen, M.-L. C. van Veelen, and G. V. Roshchupkin, "Three-dimensional stereophotogrammetry in the evaluation of craniosynostosis: Current and potential use cases," *Journal of Craniofacial Surgery*, vol. 32, no. 3, 2021.

[17] C. Elkhill, J. Liu, M. G. Linguraru, S. LeBeau, D. Khechoyan, B. French, and A. R. Porras, "Geometric learning and statistical modeling for surgical outcomes evaluation in craniosynostosis using 3d photogrammetry," *Computer Methods and Programs in Biomedicine*, vol. 240, p. 107689, 10 2023.

[18] W. E. Lorensen and H. E. Cline, "Marching cubes: A high resolution 3d surface construction algorithm," *ACM SIGGRAPH Computer Graphics*, vol. 21, pp. 163–169, 8 1987.

[19] A. Radford, L. Metz, and S. Chintala, "Unsupervised representation learning with deep convolutional generative adversarial networks," 1 2016. arXiv:1511.06434 [cs].

[20] Y. Ganin, E. Ustinova, H. Ajakan, P. Germain, H. Larochelle, F. Laviolette, M. Marchand, and V. Lempitsky, "Domain-adversarial training of neural networks," *arXiv.org*, 2016. publisher-place: Ithaca publisher: Ithaca: Cornell University Library, arXiv.org.

[21] I. Gulrajani, F. Ahmed, M. Arjovsky, V. Dumoulin, and A. C. Courville, "Improved training of wasserstein gans," vol. 30, Curran Associates, Inc., 2017.

[22] Y. Wang, Y. Feng, L. Zhang, Z. Wang, Q. Lv, and Z. Yi, "Deep adversarial domain adaptation for breast cancer screening from mammograms," *Medical Image Analysis*, vol. 73, p. 102147, 10 2021.